Structure and Thermotropic Properties of Hydrated 1-Eicosyl-2-dodecyl-*rac*-glycero-3-phosphocholine and 1-Dodecyl-2-eicosyl-*rac*-glycero-3-phosphocholine Bilayer Membranes†

J. Mattai,‡ N. M. Witzke,§ R. Bittman,§ and G. G. Shipley*,‡

Departments of Medicine and Biochemistry, Biophysics Institute, Boston University School of Medicine, Boston, Massachusetts 02118, and Department of Chemistry, Queens College, City University of New York, Flushing, New York 11367

Received May 14, 1986; Revised Manuscript Received October 14, 1986

ABSTRACT: The ether-linked phosphatidylcholines 1-eicosyl-2-dodecyl-*rac*-glycero-3-phosphocholine (EDPC) and 1-dodecyl-2-eicosyl-*rac*-glycero-3-phosphocholine (DEPC) have been investigated by differential scanning calorimetry (DSC) and X-ray diffraction. DSC of hydrated EDPC shows a single endothermic transition at 34.8 °C (ΔH = 11.2 kcal/mol) after storage at −4 °C while DEPC shows three endothermic transitions at 7.7 and ~9.0 °C (combined $\Delta H \sim$ 0.4 kcal/mol) and at 25.2 °C (ΔH = 4.7 kcal/mol). Both the single transition of EDPC and the two higher temperature transitions of DEPC are reversible, while the ~7.7 °C transition of DEPC increases in enthalpy on low-temperature incubation. At 23 °C, X-ray diffraction of hydrated EDPC shows a sharp reflection at 4.2 Å together with lamellar reflections corresponding to a bilayer periodicity, d = 56.2 Å. Electron density profiles derived from swelling experiments show a phosphate–phosphate intrabilayer distance, d_{p-p}, of 36 Å at all hydrations. This, together with calculated lipid thickness and molecular area considerations, suggests an interdigitated, three chains per head group, bilayer gel phase, L_β*, with no hydrocarbon chain tilt. This is structurally analogous to the bilayer gel phase of hydrated 18:0/10:0 ester PC [McIntosh, T. J., Simon, S. A., Ellington, J. C., Jr., & Porter, N. A. (1984) *Biochemistry 23*, 4038]. In contrast, DEPC at −4 °C shows an $L_{\beta'}$ bilayer gel phase with tilted hydrocarbon chains (d = 61.1 Å). However, this transforms above 9 °C to an interdigitated, triple-chain, L_β* bilayer gel phase (identical with that of EDPC) with d = 56.6 Å and a phosphate–phosphate distance of 36 Å. Above their respective chain melting transitions, T_m, EDPC and DEPC exhibit liquid-crystalline L_α bilayer phases with d = 64.5 and 65.0 Å at 55 and 45 °C, respectively. The ability of both EDPC and DEPC to form triple-chain interdigitated gel-state bilayers suggests that the conformational inequivalence at the *sn*-1 and *sn*-2 positions is less pronounced in the ether-linked PCs compared to the ester-linked PCs, where only one of the positional isomers, e.g., 18:0/10:0 PC but not 10:0/18:0 PC, forms the triple-chain structure (J. Mattai, unpublished results). Thus, a different conformation around the glycerol is predicted for ether-linked PC compared to ester-linked PC.

Dialkyl and monoalkyl ether-linked phospholipids are structural components of biological membranes occurring in animal cells and certain microorganisms. For example, dialkylglycerol phospholipids are the major phospholipids of *Halobacterium cutirubrum* (Sehgal et al., 1962), a halophilic bacterium, and also occur in human heart (Popović, 1965), rat brain, and ox heart (Marinetti et al., 1959). Further, mixed alkyl–acyl phospholipids such as 1-*O*-1′-alkenyl-2-acylglycerophosphocholine (plasmalogen) are also found in the brain and myelin membranes (Rouser & Yamamoto, 1968; Norton, 1981) and in malignant cells (Howard et al., 1972). While the more abundant ester-linked phospholipids in biological membranes (phosphatidylcholines and phosphatidylethanolamines) have been extensively studied, the biological significance of the ether-linked phospholipids is still unclear, and their structural properties are the subject of current investigation.

The change from an ester to an ether linkage at the glycerol backbone of certain phospholipids can affect hydrocarbon chain packing in these analogues. For example, when the alkyl and acyl chains are attached via glycerol to a phosphorylethanolamine head group, in dipalmitoylphosphatidylethanolamine (DPPE) and dihexadecylphosphatidylethanolamine (DHPE), there is an increase (~5 °C) in the gel to liquid-crystalline phase transition (Vaughan & Keough, 1974; Boggs et al., 1981) and a decrease in the liquid-crystalline to hexagonal transition (Boggs et al., 1981) for DHPE. These observations were confirmed in more detailed calorimetric and X-ray diffraction studies by Seddon et al. (1983, 1984) for a series of dialkyl- and diacylphosphatidylethanolamines. The hydrocarbon chains in the ether-linked phosphatidylethanolamines are packed closer, thus increasing the strength of intermolecular hydrogen bonding at the polar group; in addition, the ether linkage destabilizes the lamellar liquid-crystalline phase, permitting the hexagonal phase to form at a lower temperature (Seddon et al., 1983, 1984).

In contrast to the PE studies, phosphatidylcholines containing an ether or an ester linkage at the glycerol backbone appear not to show significant differences in chain packing, at least as evidenced by a lack of major changes in the chain melting transition. Differential scanning calorimetry (DSC) of 1,2-dihexadecyl-*sn*-glycero-3-phosphocholine (DHPC) by a number of workers (Vaughan & Keough, 1974; Bittman et al., 1981; Ruocco et al., 1985a), as well as fluorescence studies by Lee and Fitzgerald (1980), has shown that the ether-linked phospholipid displayed a slightly higher transition temperature (~2 °C) than the corresponding ester analogue, 1,2-di-

† This research was supported by Research Grant HL-26335 and Training Grant HL-07291 from the National Institutes of Health.

‡ Boston University School of Medicine.

§ City University of New York.

0006-2960/87/0426-0623$01.50/0

palmitoyl-*sn*-glycero-3-phosphocholine (DPPC), suggesting only small chain packing differences between these analogues. Other physical studies show little difference between these two types of phospholipids. For example, surface pressure measurements by Paltauf et al. (1971) on monolayers of dialkyl- and diacylphosphatidylcholines suggest that the molecular packing in fully expanded or condensed monolayers is not significantly different between these two analogues. ^{31}P NMR powder spectra of aqueous dispersions of DPPC and DHPC were found to be identical below (gel) and above (liquid-crystalline) the main transition temperature, T_m (Hauser, 1981). Therefore, the average conformation and segmental motion of the polar head group of the two analogues are equivalent. ^{1}H spin–spin measurements on short-chain dialkyl- and diacylphosphatidylcholines which form micelles in aqueous solutions above the critical micellar concentration also show very little difference in their conformation and motion of the glycerophosphocholine groups (Hauser et al., 1981). Further, ^{14}N spin–lattice relaxation time measurements indicated that the rate of molecular motion of the head groups is independent of the type of hydrocarbon chain linkage (Siminovitch et al., 1983). The "rippled" $P_{\beta'}$, gel L_β, and liquid-crystalline L_α phases of DHPC gave line shapes and spin–lattice relaxation times, obtained from ^{2}H NMR of polar group deuteriated DHPC, which are similar to the corresponding phases of DPPC (Ruocco et al., 1985b).

While the above results suggest that conformational and motional effects of the glycerophosphocholine groups are independent of hydrocarbon chain linkage, differences in the head-group and chain regions do exist between dialkyl- and diacylphosphatidylcholine. For example, ^{14}N NMR quadrupolar splitting of the ether-linked phospholipid in the liquid-crystalline phase is greater than in the corresponding phase of the ester-linked analogue (Siminovitch et al., 1983). ^{2}H NMR of DHPC, deuteriated in the α-methylene segments of the hydrocarbon chains, shows four quadrupolar splittings in the liquid-crystalline phase, compared to three quadrupolar splittings of the acyl derivative DPPC, indicative of different conformations in the "interfacial" region (Ruocco et al., 1985b).

Perhaps the most striking difference between the ester- and ether-linked phosphatidylcholines is in their low-temperature phases. Ruocco et al. (1985a) have shown that DHPC exists as an interdigitated lamellar gel phase at all temperatures below the pretransition, with a reversible low enthalpy transition occurring at low temperatures. In contrast, DPPC exists as a regular gel phase (not interdigitated) below the pretransition, and on annealing at low temperatures, a conditionally reversible subtransition with appreciable enthalpy is observed due to formation of a "crystalline" L_c bilayer structure (Chen et al., 1980; Füldner, 1981; Ruocco & Shipley, 1982a,b). In addition, ^{31}P NMR shows fast axial diffusion of DHPC down to −20 °C while this motion is frozen out at ~0 °C for DPPC (Ruocco et al., 1985a). While these major differences in structure occur for ether- and ester-linked phosphatidylcholines with saturated hydrocarbon chains in their low-temperature phase, little structural difference is observed for these analogues when the hydrocarbon chains are unsaturated (Schwarz et al., 1976). However, the bilayer repeat distance measurements of Schwarz et al. (1976) were made at room temperature where these lipids are in their liquid-crystalline L_α phase and not their gel phases.

As a result of a change from an ester to an ether linkage at the glycerol backbone, structural differences between these analogues are observed, especially at temperatures below T_m. In the present study, we have investigated the structural and thermotropic behavior of two highly asymmetric ether-linked isomeric phosphatidylcholines, 1-eicosyl-2-dodecyl-*rac*-glycero-3-phosphocholine (EDPC) and 1-dodecyl-2-eicosyl-*rac*-glycero-3-phosphocholine (DEPC), at different hydrations, both of these lipids containing saturated hydrocarbon chains, using the techniques of differential scanning calorimetry (DSC) and X-ray diffraction. The low-temperature phases of these ether-linked isomers are examined, and the structural data are discussed in comparison with the structures of other asymmetric and symmetric ester- and ether-linked phospholipids. Our structural results suggest that the conformation around the glycerol backbone of the ether-linked phosphatidylcholines is different from that of ester-linked phosphatidylcholines.

Materials and Methods

Materials

Materials for the synthesis of the mixed-chain ether–glycerophosphocholines EDPC and DEPC were obtained from several sources: allyl bromide, trityl chloride, trifluoroacetic acid, and 1-eicosanol (Sigma Chemical Co., St. Louis, MO); 1-bromohexadecane, 2-hexadecanol, 1,2-dichloroethane, and *m*-chloroperoxybenzoic acid (Aldrich Chemical Co., Milwaukee, WI); tetrahydrofuran and dodecanol (Baker Chemical Co., Phillipsburg, NJ); 1-bromoeicosane (Pfaltz and Bauer, Inc., Stamford, CT); 1-bromododecane (Chem Service, Media, PA); dimethyl sulfoxide and pyridine (Fisher Scientific, Rochester, NY); toluene and chloroform (MCB, Secaucus, NJ); triethylamine (Eastman Kodak Co., Rochester, NY); calcium chloride (Ventron, Danvers, MA); and silica gel 60–200 mesh (Baker Chemical Co., Phillipsburg, NJ) or silica gel 230–400 mesh (Merck and Co., Inc., St. Louis, MO).

Methods

Synthesis of the Racemic Mixed-Chain Ether-Linked Glycerophosphocholines DEPC and EDPC. The syntheses of DEPC and EDPC have been described elsewhere (Witzke & Bittman, 1986). Briefly, DEPC was prepared in a reaction sequence that began with the alkylation of 1-dodecanol with allyl bromide in the presence of sodium hydride in dimethyl sulfoxide. After hydroxylation of dodecyl allyl ether, the primary hydroxyl group was protected by tritylation. Etherification of 1-*O*-dodecyl-3-*O*-trityl-*rac*-glycerol at the C2 hydroxyl group was carried out with 1-bromoeicosane in refluxing toluene containing an excess of potassium hydroxide. Removal of the trityl group afforded 1-*O*-dodecyl-2-*O*-eicosyl-*rac*-glycerol. The phosphocholine product DEPC was obtained by reaction with phosphorus oxychloride in alcohol-free chloroform containing dry triethylamine, followed by reaction with choline tosylate in dry pyridine. The isomer EDPC was synthesized in a sequence starting with eicosyl allyl ether, which was prepared from 1-eicosanol, allyl bromide, and sodium hydride in dry dimethyl sulfoxide/tetrahydrofuran. Hydroxylation of the double bond with *m*-chloroperbenzoic acid, followed by treatment with trifluoroacetic acid and then ammonium hydroxide in a mixture of chloroform and ethanol, gave 1-*O*-eicosyl-*rac*-glycerol. Tritylation resulted in 1-*O*-eicosyl-3-*O*-trityl-*rac*-glycerol, and etherification of the hydroxyl group at C2 with 1-bromododecane and potassium hydroxide in refluxing toluene gave 1-*O*-eicosyl-2-*O*-dodecyl-3-*O*-trityl-*rac*-glycerol. After removal of the trityl group, the phosphocholine product EDPC was obtained by reaction with phosphorus oxychloride and choline tosylate, as described above for the DEPC isomer. Elemental analyses and ^{1}H NMR

spectral data were consistent with the proposed structures [see Witzke & Bittman (1986) for experimental details].

DSC and X-ray Diffraction. For DSC studies, the ether lipids were weighed directly into stainless-steel pans, and ~90 wt % water was added with a Hamilton syringe. The pans were hermetically sealed and transferred to the scanning calorimeter (Perkin-Elmer, Norwalk, CT). After several heating and cooling cycles over the temperature range −4 → 45 °C, the samples were incubated at −4 °C for periods greater than 2 weeks. This was followed by a cold transfer of the sample to the calorimeter, preset at −4 °C, and heating, cooling, and reheating thermograms were obtained. In some instances, incubation for shorter periods of time was performed to monitor any enthalpic changes due to possible formation of low-temperature phases.

For X-ray diffraction measurements, dried samples were weighed directly into quartz capillary tubes (internal diameter = 1 mm) (Charles Supper Co., Natick, MA), and water was added gravimetrically to produce samples at different hydrations. The sample tubes were flame-sealed, inserted in a glass centrifugation tube padded at the bottom with tissue paper, and equilibrated by repeated centrifugation at ~3200 rpm above T_m for 1–2 h using a clinical centrifuge (Damon, IEC, MA). After storage at −4 °C for several weeks, the samples were cold-transferred to the X-ray sample holder, preset at −4 °C. X-ray diffraction patterns were recorded with photographic film using nickel-filtered Cu Kα X-radiation from an Elliot GX-6 rotating anode generator (Elliot Automation, Borehamwood, England), which was collimated by double-mirror optics or toroidal optics into a point source. X-ray diffraction patterns were also recorded with a position-sensitive proportional detector. Cu Kα radiation from a microfocus X-ray generator (Jarrell-Ash, Waltham, MA) was line-focused (100 μm × 14 mm) by a single mirror and collimated with the slit optical system of a Luzzati–Baro camera. X-ray diffraction patterns were recorded by using a linear position sensitive detector (Tennelec, Oak Ridge, TN) and associated electronics (Tracor Northern, Middleton, WI). Samples were mounted in a variable-temperature sample holder with a temperature stability of ±1 °C. Microdensitometry of X-ray diffraction photographs was carried out with a Joyce Loebl Model III-CS microdensitometer.

Results and Discussion

Thermotropic and Structural Behavior of Hydrated EDPC

Differential Scanning Calorimetry (DSC). DSC of hydrated (90 wt % water) EDPC after incubation at −4 °C for 61 days shows a single sharp endothermic transition at 34.8 °C (ΔH = 11.2 kcal/mol) (Figure 1a). On cooling, two exothermic transitions are observed (Figure 1b): a sharp transition at 30.5 °C and a broader transition at 26.2 °C with a shoulder at 27.7 °C. The total enthalpy of the exothermic transition is 10.9 kcal/mol; hence almost the total enthalpy is recovered on cooling. On immediate reheating (Figure 1c), only the single sharp endothermic transition at 34.8 °C is observed with ΔH = 11.2 kcal/mol, identical with the enthalpy observed followed prolonged incubation. Thus, the transition at 34.8 °C is reversible. Clearly, EDPC does not form metastable gel phases or exhibit the pretransition observed in the more symmetric DHPC (Ruocco et al., 1985a) and other symmetric and asymmetric ester-linked phosphatidylcholines (Chen et al., 1980; Ruocco & Shipley, 1982a,b; Serrallach et al., 1984). Prolonged incubation at lower temperatures such as −8 or −16 °C also did not generate any additional low-temperature phases(s). In the next section, the structures of both the low- and high-temperature phases of hydrated EDPC are described.

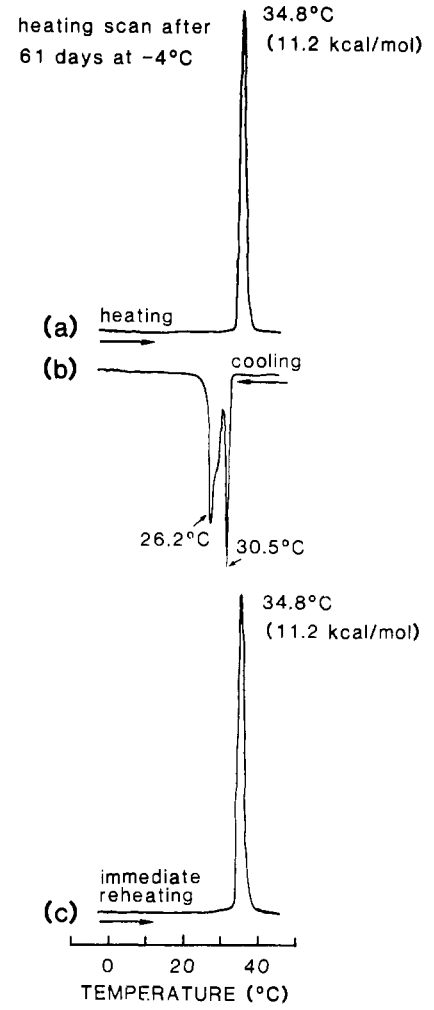

FIGURE 1: (a) DSC heating curve of hydrated (90 wt % water) EDPC after 61 days of incubation at −4 °C; (b) cooling curve; (c) immediate reheating curve. Heating and cooling rates, 5 °C/min.

X-ray Diffraction of Hydrated EDPC. After prolonged incubation at −4 °C, X-ray diffraction patterns of hydrated (54 wt % water) EDPC were recorded at −2, 23, and 40 °C. The X-ray diffraction pattern at −2 °C was found to be identical with that at 23 °C, demonstrating the absence of sub-gel phase formation at low temperatures. In Figure 2a, the X-ray diffraction pattern at 23 °C shows five low-angle reflections; the first three reflections (h = 1 → 3) are strong, while the fourth and fifth orders are weak. These reflections index in the ratio $1:{}^1/_2:{}^1/_3:{}^1/_4:{}^1/_5$, ..., consistent with a lamellar phase with a bilayer periodicity, d = 56.2 Å. The wide-angle region (see Figure 2a) shows a single sharp symmetric reflection at 4.2 Å indicative of a gel phase with the hydrocarbon chains packed in a hexagonal arrangement perpendicular to the bilayer plane; there is no evidence of hydrocarbon chain tilt (Tardieu et al., 1973). At 40 °C (Figure 2b), three broad lamellar reflections, d = 68.9 Å, are observed in the low-angle region. The wide-angle region shows a single diffuse reflection at 4.5 Å, characteristic of the liquid-crystalline L_α bilayer phase.

Figure 3a,b shows X-ray diffraction patterns of hydrated (54 wt % water) EDPC as a function of increasing and decreasing temperatures using a linear position sensitive detector. The initial diffraction pattern at −4 °C (Figure 3a), obtained after prolonged incubation at −4 °C, shows lamellar reflections

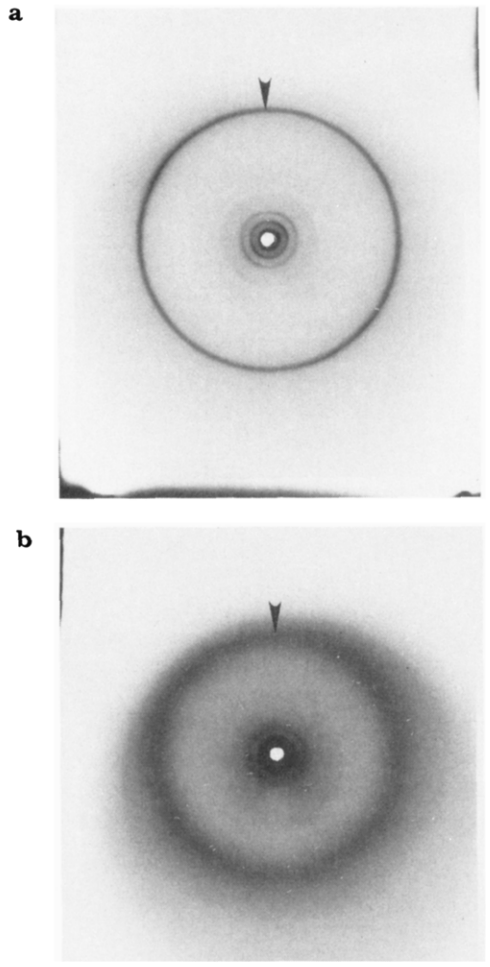

FIGURE 2: X-ray diffraction patterns recorded by using toroidal optics of hydrated (54 wt % water) EDPC after 21 days of incubation at −4 °C. (a) 23 and (b) 40 °C. Arrows correspond to wide-angle reflections noted in the text.

in the low-angle region (d = 56.2 Å) with the single sharp symmetric 4.2-Å reflection in the wide-angle region, consistent with the X-ray diffraction pattern described above (see Figure 2a). On heating at 3.5 °C intervals, both the low- and wide-angle reflections remain essentially constant until 34.5 °C, at which temperature two changes occur; first, the low-angle reflections become more diffuse but still consistent with a lamellar bilayer geometry, d = 68.9 Å, and second, the wide-angle reflection shifts and broadens to give the 4.5-Å reflection characteristic of the melted chain L_α phase. The diffraction patterns did not change on further heating to 41.5 °C. It is clear that at low temperatures, no subgel formation occurs. On cooling (Figure 3b), the diffuse 4.5-Å wide-angle reflection changes to the sharp 4.2-Å reflection at 27.5 °C, and this reflection persists down to −4 °C; the low-angle lamellar reflections also change at 27.5 °C to give a bilayer periodicity d = 56.2 Å, this value remaining essentially constant down to −4 °C.

Below the main transition temperature, X-ray diffraction patterns of fully hydrated EDPC are similar to the patterns observed for the highly asymmetric ester-linked 1-stearoyl-2-caproyl-*sn*-glycero-3-phosphocholine (SCPC) (McIntosh et al., 1984; Hui et al., 1984). Below T_m and at maximum hydration, SCPC showed a single wide-angle reflection at 4.11 Å and several lamellar reflections (d = 59.3 Å). The X-ray diffraction pattern of SCPC was analyzed to show that three hydrocarbon chains exist per polar head group in a mixed interdigitated arrangement spanning the bilayer. This gel phase, with three hydrocarbon chains per polar head group, which we will designate as L_β*, occurs because the stearoyl chains of SCPC are able to span the bilayer while the caproyl chains from one monolayer are aligned with caproyl chains from the apposing monolayer. Such an arrangement is energetically favorable because the length of one stearoyl chain is equivalent to the length of two caproyl chains especially when the bend in the *sn*-2 chain is taken into account (Hitchcock et al., 1974).

Since a similar asymmetry in the number of carbon atoms of the hydrocarbon chains exists in EDPC and SCPC, additional swelling experiments by X-ray diffraction were performed on EDPC to determine whether the L_β* phase also exists for this ether-linked phospholipid. Diffraction patterns were obtained over the concentration range 25.9–54.0% water at 23 °C. The single sharp wide-angle reflection at 4.2 Å is observed at all hydrations, while changes were observed in both the intensity and lamellar repeat distances of the low-angle reflections. Figure 4a shows the hydration dependence of the lamellar repeat distance (d) together with other structural parameters, lipid thickness (d_l) and surface area per lipid molecule (S), calculated from d by using the equations of Luzzati (1968). The bilayer repeat distance is observed to increase from 50.9 Å at 25.9% water reaching a limiting value at 56.6 Å at ~35% hydration, after which no further changes in d are observed. The limiting hydration corresponds to 21 molecules of water bound per EDPC molecule. The calculated lipid thickness and surface area remain approximately constant at 36–37 Å and 60 Å^2, respectively, over this hydration range (see Figure 4a). This lipid thickness was calculated by using the assumption that the partial specific volume, $\bar{v}$, of EDPC is 0.936 cm^3/g, the value for gel-phase dipalmitoylphosphatidylcholine at 23 °C (Nagle & Wilkinson, 1978).

The intensities of the low-angle reflections were used to determine the structure amplitudes over the hydration range 25.9–54.0%. This is the standard swelling method [see, for example, Torbet & Wilkins (1976), Janiak et al. (1979), McDaniel et al. (1983), Mattai & Shipley (1986), and McIntosh & Simon (1986)] for determining the continuous transform from which the phases of the structure amplitudes are determined. This assumes that the bilayer structure is independent of hydration [although see Torbet & Wilkins (1976)]. For all samples, the observed intensities were corrected for Lorentz and polarization factors ($I_{00l} \times l^2$) and normalized with respect to each other according to standard procedures (Worthington & Blaurock, 1969). The normalized amplitudes are plotted as a function of the reciprocal space coordinate s ($s = 2 \sin\theta/\lambda$) as shown in Figure 5a. The nodes, i.e., the points at which a phase change could occur, are suggested by the amplitude data and confirmed by application of the Shannon sampling theorem (Shannon, 1949). This indicated that phase changes occur at s = 0.008, 0.042, and 0.067 Å^{-1}. For all hydrations, the phase sequence for l = 1–5 was − − + − −, and the corresponding electron density profiles are shown in Figure 6a. The region of high electron density at ±18 Å, corresponding to the electron-rich phosphate–phosphate intrabilayer distance, d_{p-p},[1] of 36 Å, is independent of hydration. This intrabilayer distance is similar to the phosphate–phosphate distance determined for other interdi-

[1] We recognize that electron density profiles at this resolution probably provide an underestimate of the true phosphate–phosphate separation across the bilayer [see, for example, Hitchcock et al. (1974) for an example of this problem]. However, we prefer to use the term d_{p-p} to describe the separation of the electron-dense regions across the bilayer due to the location of the phosphate groups.

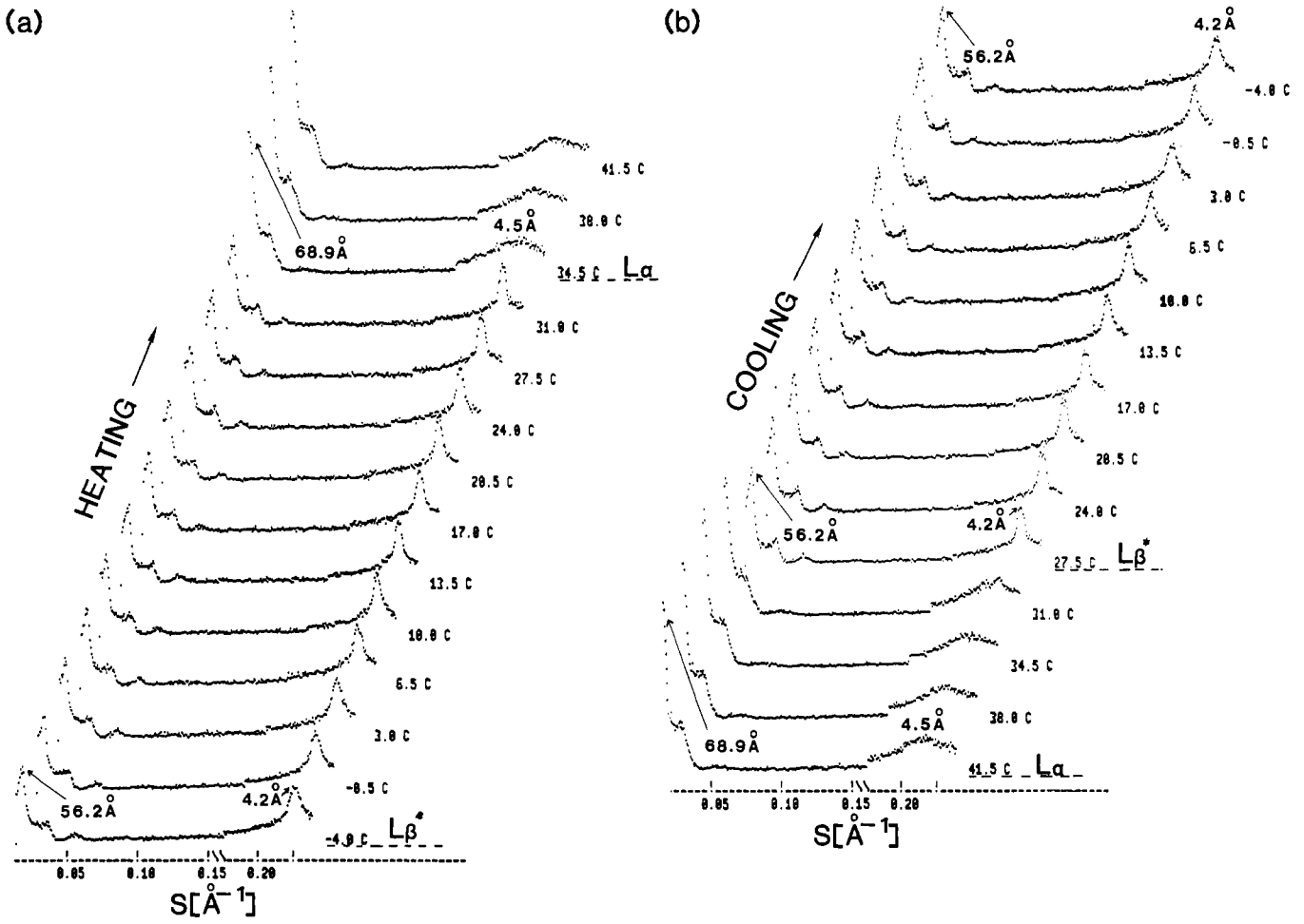

FIGURE 3: X-ray diffraction patterns of hydrated (54 wt % water) EDPC as a function of increasing (a) and decreasing (b) temperatures. EDPC was incubated at −4 °C for several weeks prior to the heating run. Intensity data were recorded by using a linear position sensitive detector, with an acquisition time of 10 min at each temperature.

gitated gel phases (Serrallach et al., 1983; McIntosh et al., 1984; Ruocco et al., 1985a). A d_{p-p} distance of 36 Å is too short for a regular interdigitated bilayer with the 20-carbon chain directly apposed by the 12-carbon chain and the hydrocarbon chains perpendicular to the bilayer normal (as indicated by the single sharp 4.2-Å reflection; see Figure 2a).

The combination of the wide-angle diffraction data and the electron density profiles suggests that fully hydrated EDPC below the phase transition temperature exists with its hydrocarbon chains interdigitated. It is necessary to resolve whether this interdigitation is of the "monolayer" type, whereby four hydrocarbon chains exist per lipid head group (Ranck et al., 1977; Serrallach et al., 1983; McDaniel et al., 1983; Ruocco et al., 1985a), or of the mixed interdigitated bilayer type L_β*, like that of hydrated SCPC (McIntosh et al., 1984; Hui et al., 1984). In the latter arrangement, three hydrocarbon chains exist per lipid head group. Using the wide-angle reflection data shown in Figure 2a, we have calculated the area per hydrocarbon chain of EDPC at different degrees of hydration to be $\sum = 20.4$ Å^2, below T_m, using the formula $\sum = 2d^2/3^{1/2}$ (Tardieu et al., 1973). The average area available to one EDPC molecule at the phospholipid–water interface, S, is calculated to be ~60 Å^2 [Figure 4a; see Luzzati (1968) for this approach]. Therefore, $S/\sum \sim 3.0$, indicating that three hydrocarbon chains are occupied per lipid head group in hydrated EDPC below T_m at all hydrations. These results indicate that below T_m, the hydrocarbon chains of EDPC exist in a mixed interdigitated arrangement like that of SCPC (McIntosh et al., 1984; Hui et al., 1984). In this case, the eicosyl chains span the width of the bilayer, and the dodecyl chains from opposing leaflets of the bilayer pack end to end to give three hydrocarbon chains per head group (see Figure 7). McIntosh et al. (1984) have indicated that this type of interdigitation for SCPC is facilitated because the stearoyl chains are approximately twice the length of the decanoyl chains, permitting an energetically favorable packing of the hydrocarbon chains with optimal van der Waals interactions.[2] Apparently, a similar mismatch between the eicosyl and dodecyl hydrocarbon chains of EDPC also exists, thus enabling the formation of the mixed interdigitated gel phase, L_β*. Note that the location of the juxtaposed 12-carbon chains should produce lower electron density at the bilayer center (as observed in Figure 6a), although a more pronounced trough at the bilayer center should be observed for noninterdigitated symmetric bilayers. This mismatch of hydrocarbon chains allows formation of a *stable* L_β* phase for EDPC, which does not transform into subgel phases after months of low-temperature incubation.

Swelling experiments were also performed at 55 °C to determine the structural changes of the liquid-crystalline phase on hydration. The difraction patterns in the wide-angle region

[2] Obviously in the triple-chain interdigitated structure the methyl groups of the eicosyl chains are located near the lipid interface. Although this aspect of the structure is presumably energetically unfavorable, it must be outweighed by the energetically favorable arrangement provided by the chain packing [see McIntosh et al. (1984) for a detailed discussion of this issue].

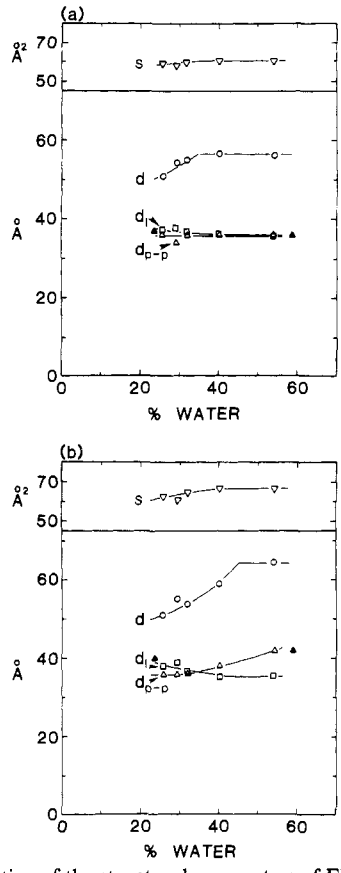

FIGURE 4: Variation of the structural parameters of EDPC with water content at (a) 23 and (b) 55 °C. (○) Bilayer repeat distance, d; (□) lipid thickness, d_l; (△) phosphate–phosphate distance, d_{p-p}; (▽) area of one EDPC molecule at the lipid–water interface, S. Solid symbols are d_{p-p} values for DEPC at (a) 14 and (b) 45 °C; see text.

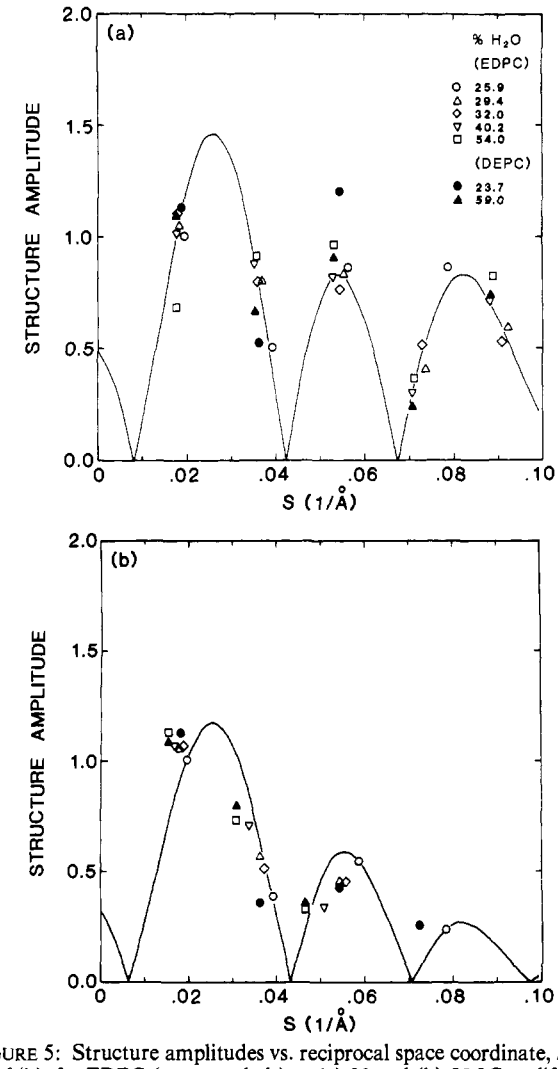

FIGURE 5: Structure amplitudes vs. reciprocal space coordinate, s (=2 sin θ/λ), for EDPC (open symbols) at (a) 23 and (b) 55 °C at different degrees of hydration. Solid symbols are for DEPC at (a) 14 and (b) 45 °C; see text. The solid lines are transforms calculated by using Shannon's sampling theorem (see text) for 40.2% and 25.9% hydrated EDPC at 23 and 55 °C, respectively.

over the hydrated range 25.9–54.0% gave a single broad reflection at 4.5 Å, confirming the presence of the L_α phase at 55 °C. The lamellar repeat distance, calculated lipid thickness (d_l), and surface area per lipid head group (S) are shown as a function of increasing water content in Figure 4b. The bilayer repeat distance increased from 51.1 Å at 25.9% hydration to a limiting value of 64.5 Å at approximately 45% water content. The lipid thickness, d_l, was calculated as previously described, assuming a partial specific volume of 1.01 cm/g for EDPC in the L_α phase corresponding to $\bar{v}$ of dipalmitoylphosphatidylcholine in the L_α phase (Nagle & Wilkinson, 1978). d_l is observed to decrease from 38 Å at 25.9% water to 35.5 Å at maximum hydration, while the surface area per lipid head group correspondingly increases from 62 to 66–67 Å^2.

Structure amplitudes were calculated for EDPC at 55 °C in the L_α phase. Four reflections were observed for the 25.9% hydrated sample, while the other hydrated samples gave only three reflections. The corrected and normalized amplitudes at all hydrations are shown in Figure 5b as a function of the reciprocal space coordinate s. Nodes corresponding to phase changes are evident at 0.007, 0.043, and 0.071 Å^{-1}, and, hence, the phase assignments are $--+-$ for the 25.9% hydrated sample and $--+$ for the higher hydration samples. The low-resolution profiles, shown in Figure 6b, show a well-defined trough of low electron density corresponding to the bilayer center while the regions of high electron density gave phosphate–phosphate distances which change from 36 Å at 25.9% hydration to 42 Å at 54% hydration. In contrast, the calculated lipid thickness is shown to decrease slightly from 38 to 35.6 Å and the surface area to increase slightly from 62.2 to 66.4 Å^2 over a similar hydration range. Although it is difficult to resolve this inconsistency in the hydration dependence of d_l and d_{p-p}, the electron density profiles might suggest that the bilayer structure is changing with hydration. However, both the lipid thickness and the surface area data are similar to those of other melted "two-chain" L_α bilayers (Luzzati, 1968). Thus, a regular melted two-chain L_α phase is present at higher hydration. While the electron density profiles (Figure 6b) show no strong evidence for interdigitation in the L_α phase, the high degree of asymmetry of the hydrocarbon chains in EDPC suggests that partial interdigitation (see Figure 7) must occur to avoid packing problems in the geometric center of the bilayer.

In Figure 7, a schematic representation of the structural changes of fully hydrated EDPC is shown. Below 34.8 °C, a stable three-chain interdigitated bilayer gel phase, L_β*, exists with the hydrocarbon chains packed perpendicular to the bilayer plane. At 34.8 °C, the L_β* phase converts to the liquid-crystalline L_α bilayer phase with the melted hydrocarbon chains aligned approximately perpendicular to the bilayer phase. On cooling, the L_α phase reverts to the stable L_β* phase with little or no supercooling. The structural changes occurring between the two exothermic transitions observed on cooling (see Figure 1b) have not been elucidated.

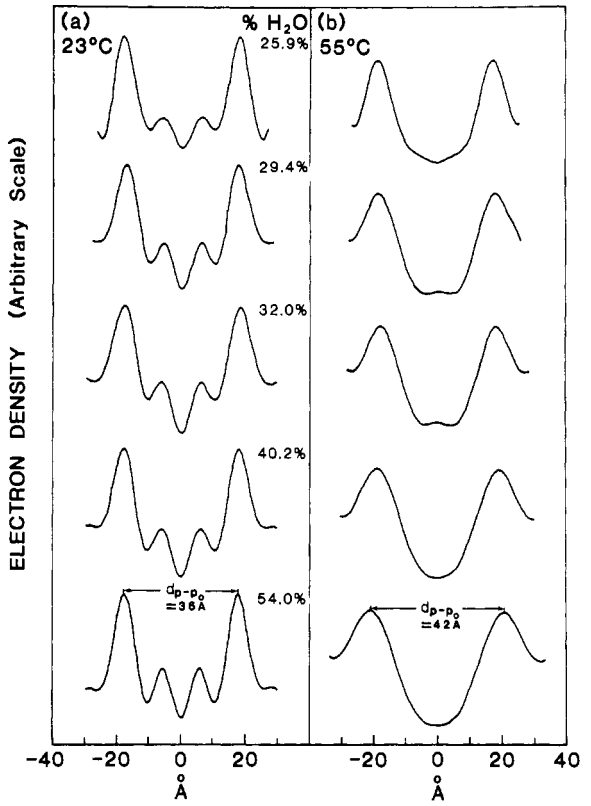

FIGURE 6: Electron density profiles of EDPC at different hydrations at (a) 23 and (b) 55 °C.

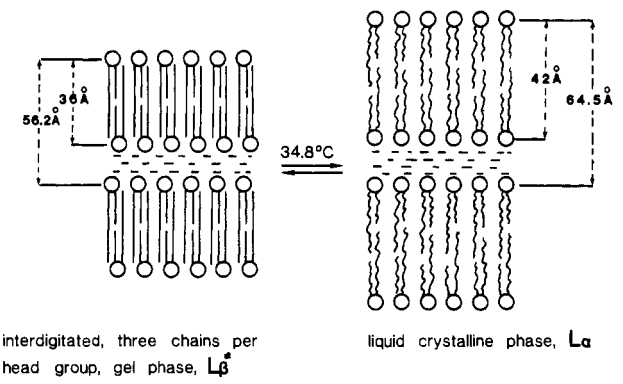

FIGURE 7: Schematic representation of the structural changes exhibited by hydrated EDPC.

Thermotropic and Structural Behavior of Hydrated DEPC

Differential Scanning Calorimetry. Hydrated (90 wt % water) DEPC, after prolonged incubation at −4 °C, shows three endotherms at 7.7 and 9.0 °C (combined $\Delta H \sim 0.4$ kcal/mol) and at 25.0 °C ($\Delta H = 4.7$ kcal/mol) (see Figure 8a). On cooling (Figure 8b), two transitions are observed, a sharp exotherm at 21 °C ($\Delta H = 4.1$ kcal/mol) and a broader low-temperature transition at 3 °C ($\Delta H = 0.3$ kcal/mol). Immediate reheating (Figure 8c) produced two endothermic transitions at 9 and 25.0 °C ($\Delta H = 4.7$ kcal/mol); these two transitions are evidently reversible. The endotherm at 7.7 °C is not reversible, and it appears to be a "subtransition" which is generated following low-temperature incubation. Because of the small value of ΔH (<0.4 kcal/mol) for this low-temperature transition, we were unable to monitor the kinetics of its formation; however, overnight incubation (~16 h) at −4 °C was sufficient to produce the 7.7 °C transition. Since the enthalpy is small compared to the enthalpy of sub-gel phase

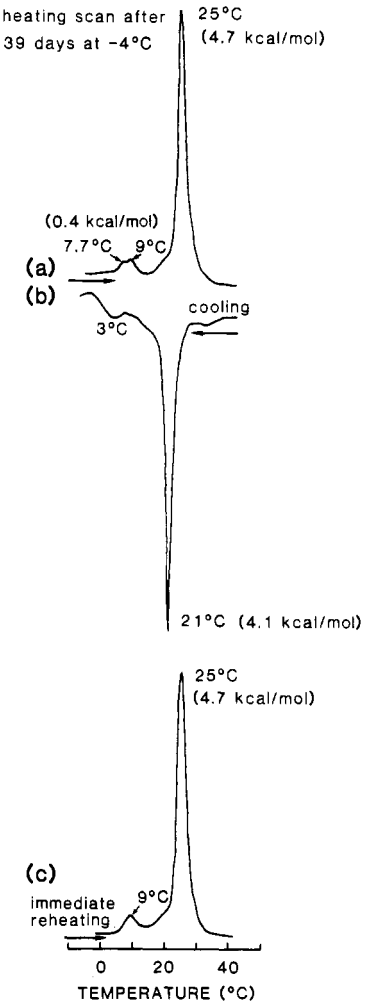

FIGURE 8: (a) DSC heating curves of hydrated (90 wt % water) DEPC after 39-days incubation at −4 °C; (b) cooling curve; (c) immediate reheating curve. Heating and cooling rates, 5 °C/min.

formation of other symmetric and asymmetric ester-linked phosphatidylcholines (Chen et al., 1980; Füldner, 1981; Ruocco & Shipley, 1982a,b; Serrallach et al., 1983, 1984; Stümpel et al., 1983), we suspect that it does not reflect formation of an ordered "L_c-type" phase (see below).

In the next section, we have attempted to characterize the various phases of hydrated DEPC at different temperatures.

X-ray Diffraction of Hydrated DEPC. X-ray diffraction patterns of fully hydrated (59 wt % water) DEPC at −4, 14, and 31 °C are shown in panels a, b, and c, respectively, of Figure 9. The X-ray diffraction pattern at −4 °C (Figure 9a), obtained after prolonged storage at −4 °C, shows six lamellar reflections ($h = 1 \rightarrow 6$) in the low-angle region corresponding to a bilayer repeat distance $d = 61.1$ Å. The first four orders are quite strong in intensity, while the fifth order is absent and the sixth order is weak. The wide-angle region shows two reflections, a sharp one at 4.3 Å and a more diffuse one at 4.1 Å. This pattern is characteristic of a gel phase, $L_{\beta'}$, with tilted hydrocarbon chains and hexagonal chain packing, as observed in other ester-linked phosphatidylcholine systems (Tardieu et al., 1973; Janiak et al., 1976, 1979). On heating to 14 °C, corresponding to a temperature between the low-temperature reversible transition at 9.0 °C and the main transition at 25.0 °C, the X-ray diffraction pattern (Figure 9b) shows five lamellar reflections, bilayer periodicity $d = 56.6$ Å; the first three orders ($h = 1 \rightarrow 3$) are quite strong while there is an absent fourth order and a weak fifth-order reflection. The wide-angle region shows a single sharp reflection

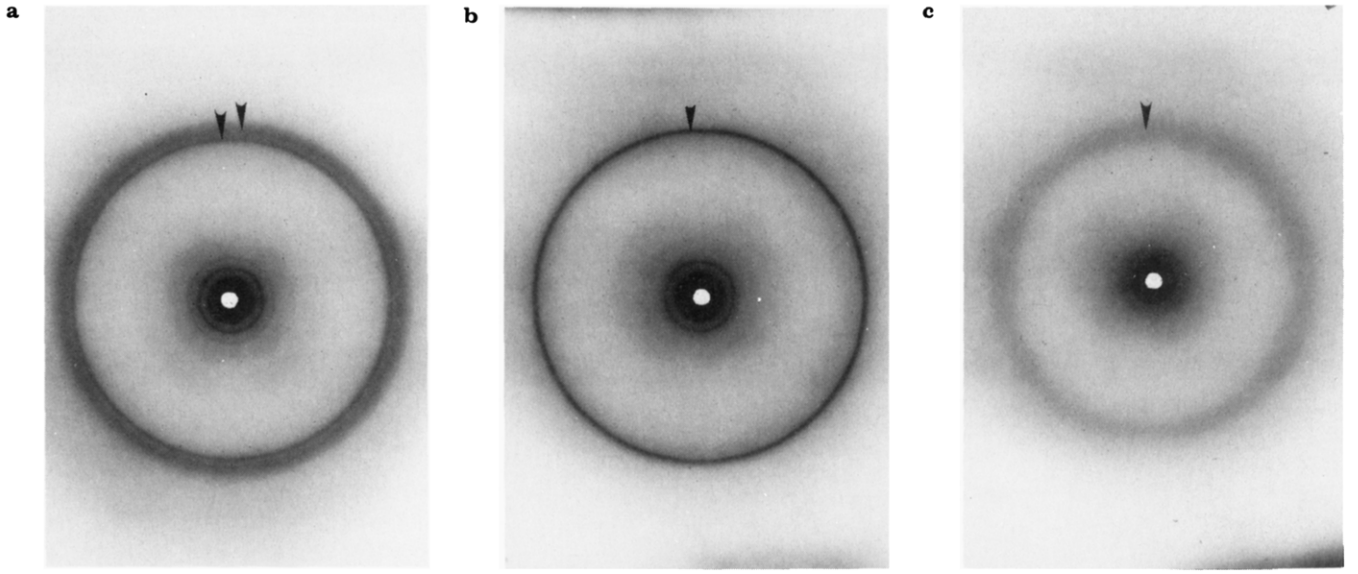

FIGURE 9: X-ray difffraction patterns recorded by using toroidal optics of hydrated (59 wt % water) DEPC after prolonged incubation at −4 °C. (a) −4, (b) 14, and (c) 31 °C. Arrows correspond to wide-angle reflections noted in the text.

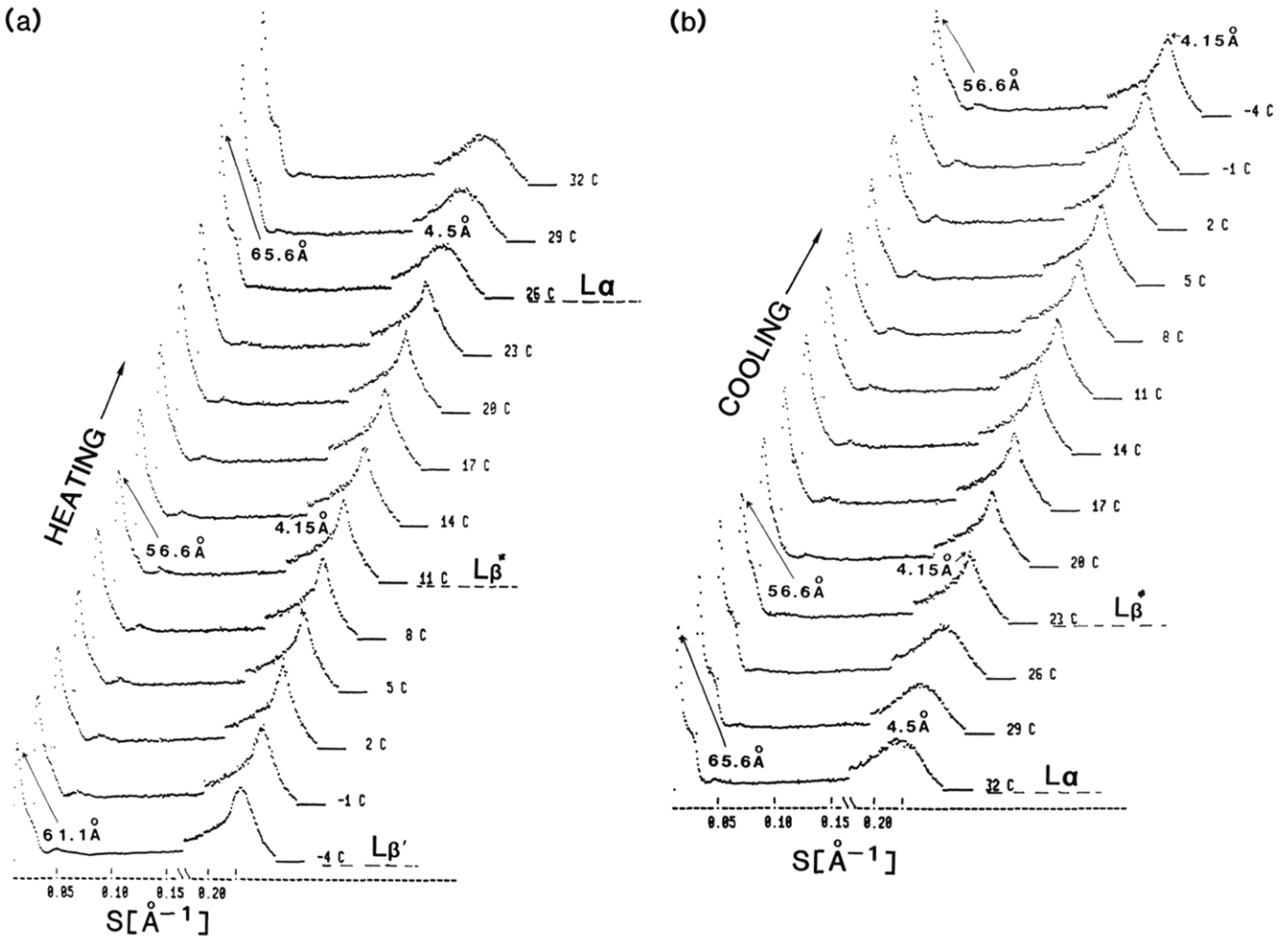

FIGURE 10: X-ray diffraction patterns of hydrated (59 wt % water) DEPC as a function of increasing (a) and decreasing (b) temperature. DEPC was incubated at −4 °C prior to the heating run. Intensity data were recorded by using a linear position sensitive detector, with an acquisition time of 10 min at each temperature.

at 4.15 Å, indicating that the hydrocarbon chains are packed in an arrangement perpendicular to the bilayer surface without chain tilting (Tardieu et al., 1973). This diffraction pattern of DEPC at 14 °C is almost identical with that of the gel phase of EDPC below its transition temperature, and we will demonstrate (see below) that DEPC, at 14 °C, also forms a mixed interdigitated, three chains per head group, gel phase, L_β*. At 31 °C, above the main transition (Figure 9c), the diffraction pattern shows lamellar reflections (h = 1–3) in the low-angle region (d = 65.6 Å) while the reflection at 4.5 Å in the wide-angle region is characteristic of the liquid-crystalline L_α phase with melted hydrocarbon chains.

Figure 10a,b shows X-ray diffraction patterns of fully hydrated DEPC as a function of increasing (−4 → 32 °C) and decreasing (32 → −4 °C) temperature using a linear position sensitive detector. At −4 °C, the low-angle region shows three lamellar reflections (d = 61.1 Å) while the wide-angle region shows a broad asymmetric reflection at ~4.0 Å. The higher order lamellar reflections, seen in Figure 9a, are absent in the patterns of Figure 10a, due to the short, 10-min acquisition time. Further, the geometry of the detector does not permit good resolution of the two wide-angle reflections at 4.31 and 4.06 Å of the chain-tilted $L_{\beta'}$ gel phase clearly visible in Figure 9a. On heating at 3 °C intervals, there is little detectable change over the next 12 °C in the low-angle reflections while the broad reflection in the wide-angle region becomes sharper. By ~11 °C, a single, sharp symmetric 4.15-Å reflection is observed in the wide-angle region, characteristic of untilted hydrocarbon chains of DEPC at this temperature (see also Figure 9b). The low-angle region shows three lamellar reflections, with d = 56.6 Å at 11 °C. So far, we have been unable to distinguish the independent structural changes attributable to the two transitions at 7.7 and 9.0 °C. Both the low- and wide-angle reflections persist up to 26 °C, at which temperature the wide-angle region shows the diffuse 4.5-Å reflection characteristic of the L_α phase. The bilayer repeat distance also changes from 56.6 to 65.6 Å at temperatures >26 °C.

On cooling, the 4.5-Å reflection of the L_α phase does not change over the temperature range 32–26 °C; below this temperature, changes occur in both the low- and wide-angle reflections. At 23 °C, the single sharp symmetric reflection at 4.15 Å characteristic of the L_β* phase with untilted hydrocarbon chains is observed, while the bilayer repeat distance in the low-angle region changes from 65.6 to 56.6 Å. The phase change at 25.2 °C (liquid crystalline, L_α → mixed interdigitated, L_β*) is clearly reversible. This type of reversible behavior ($L_\alpha \rightleftarrows L_\beta$*) was also observed for hydrated EDPC. Further cooling to −4 °C does not change either the low- or the wide-angle reflections. While the DSC cooling curve of Figure 8b shows an exotherm at 3 °C, the X-ray diffraction patterns below 3 °C do not show significant changes in the wide- or low-angle region. It appears that the low-temperature tilted chain phase, $L_{\beta'}$ of hydrated DEPC (see Figure 9a and Figure 10a at −4 °C) is not immediately generated on cooling but is obtained in a time- and temperature-dependent manner from the mixed interdigitated, L_β* phase after low-temperature incubation. We have not made a detailed study of this interconversion.

We have determined the structure factor amplitudes at two hydrations (23.7% and 59.0%) of DEPC at −4, 14, and 45 °C from the low-angle reflections at these temperatures. The amplitudes of DEPC at 14 and 45 °C are plotted (solid symbols) for comparison to EDPC in Figure 5a,b. Quite good agreement is observed from which phase assignments were deduced. The phases of the structure factors were assigned the sequence − − + − [see Torbet & Wilkins (1976) and McIntosh & Simon (1986) for phase assignments of a tilted $L_{\beta'}$ bilayer structure], − − + − − (see Figure 5a), and − − + (see Figure 5b) at −4, 14, and 31 °C, respectively, and the corresponding electron density profiles at two hydrations are shown in Figure 11a–c. The two profiles at −4 °C are essentially identical, suggesting that at 23.7% water the bilayers are fully hydrated; d_{p-p} is 42 Å, consistent with the tilted $L_{\beta'}$ structure suggested above (see Figure 12).

The electron density profiles of DEPC at 14 °C (Figure 11b) show a short d_{p-p} distance of 36 Å, together with some evidence

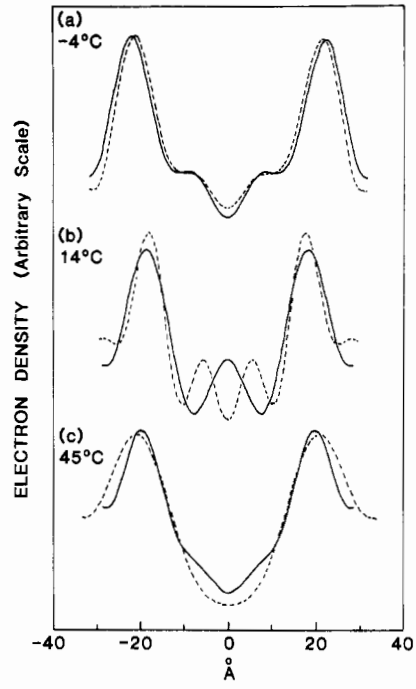

FIGURE 11: Electron density profiles of 23.7% (—) and 59.0% (- - -) hydrated DEPC at (a) −4, (b) 14, and (c) 45 °C.

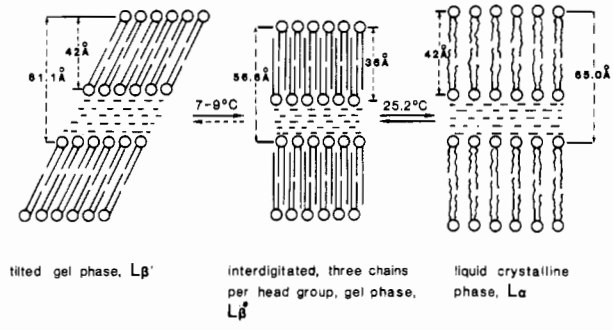

FIGURE 12: Schematic representation of the structural changes exhibited by hydrated DEPC.

of interdigitation at the bilayer center, while as shown by the wide-angle X-ray diffraction (see Figure 9b), the hydrocarbon chains of DEPC at 14 °C are perpendicular to the bilayer plane. Further, the diffraction patterns and electron density profiles of DEPC at 14 °C are essentially identical with those of hydrated EDPC below its transition temperature (compare Figures 2a and 9b as well as Figures 6a and 11b). Since the proposed structure of EDPC below T_m is a mixed, interdigitated, L_β* gel phase with three hydrocarbon chains per head group, the electron density and X-ray diffraction data suggest a similar structure for DEPC between the 9 °C transition and the chain-melting transition at 25.0 °C. To confirm this structure, we have calculated the area per hydrocarbon chain of DEPC at 14 °C to be 19.9 Å^2 while the area, S, available to one DEPC molecule at the lipid–water interface is determined to be 61 Å^2 using the same assumptions described above for EDPC. Therefore, the number of hydrocarbon chains per head group is ~3, a value identical with that found for EDPC below T_m and for ester-linked SCPC in its gel phase (McIntosh et al., 1984; Hui et al., 1984). Hence, the hydrocarbon chains of ether-linked DEPC, over the temperature range 9–25 °C, are packed in a mixed interdigitated arrangement with three hydrocarbon chains per head group (see Figure 12).

The electron density profiles of hydrated DEPC in the liquid-crystalline phase at 45 °C (Figure 11c) are different from

the profiles at 14 °C (Figure 11b). The d_{p-p} distance increases to 42 Å, and the profile shows a central trough of low electron density in the center of the bilayer. There is very little difference between the electron profiles of DEPC and EDPC in their liquid-crystalline phases (see Figures 6b and 11c). Again, the high degree of asymmetry of the hydrocarbon chains would suggest some degree of interdigitation even in the L_α phase (see Figure 12).

Figure 12 summarizes the structural behavior of hydrated DEPC. After low-temperature incubation, fully hydrated DEPC forms a tilted, interdigitated gel phase, with the 20-carbon and 12-carbon chains apposed across the bilayer center. This gel phase undergoes a low enthalpy phase change at ~7.7 °C. We have not been able to characterize the structural change accompanying this transition by X-ray diffraction. Above the 9.0 °C transition, a mixed interdigitated, three chains per head group, gel phase, L_β*, is formed, similar to that observed for hydrated EDPC below T_m and for SCPC below T_m (McIntosh et al., 1984; Hui et al., 1984). Above 25.0 °C, the L_β* phase of fully hydrated DEPC transforms to the liquid-crystalline L_α phase. On cooling, the $L_\alpha \rightarrow L_\beta$* phase change is reversible; however, the L_β* phase persists down to low temperatures; only following low-temperature incubation does it eventually transform into the tilted gel phase, $L_{\beta'}$ (cf. the two different, albeit poorly resolved, wide-angle X-ray diffraction patterns recorded at −4 °C in Figure 10a,b).

The formation of the L_β* phase, in both the ester-linked SCPC and the ether-linked EDPC and DEPC, would suggest that the difference in hydrocarbon chain lengths between the *sn*-1 and *sn*-2 positions of the glycerol backbone, and not the nature of the linkage (ester vs. ether) to the glycerol backbone, is a prerequisite for mixed hydrocarbon chain interdigitation. Raman spectroscopic studies of aqueous dispersions of synthetic DL-*erythro*-*N*-lignoceroylsphingosylphosphocholine suggest that a mixed interdigitated, L_β*, phase also exists for this highly asymmetric sphingomyelin below 48.5 °C (Levin et al., 1985). Analogous to SCPC (McIntosh et al., 1984; Hui et al., 1984), the stability of the L_β* phase of EDPC results from the fact that the length of one eicosyl chain is approximately equal to twice the length of two dodecyl chains in the ether-linked phospholipid. In the ether-linked isomer, DEPC, the L_β* phase is not the stable phase of the lipid below 7–8 °C; X-ray diffraction shows that this phase eventually transforms into a tilted $L_{\beta'}$ gel phase after low-temperature incubation. This would suggest that in DEPC, the length of two dodecyl hydrocarbon chains at the *sn*-1 positions of the glycerol backbone does not exactly match the length of the eicosyl chain at the *sn*-2 position. Therefore, the L_β* phase of DEPC would be energetically less stable than the L_β* phase of EDPC and hence is transformed into a different gel phase ($L_{\beta'}$).

Conclusions

We have demonstrated that both asymmetric ether-linked isomers, EDPC and DEPC, form the mixed, triple-chain, interdigitated bilayer gel L_β* phase. In contrast, only one of the asymmetric ester-linked isomers, SCPC, forms an L_β* phase (McIntosh et al., 1984; Hui et al., 1984), while its isomer, CSPC, forms a "crystalline" L_c phase at low temperatures (J. Mattai, unpublished results). The change in linkage at the glycerol backbone clearly affects the formation of the L_β* phase between ester- and ether-linked phosphatidylcholines.

Recent studies (Ruocco et al., 1985a) have shown even more drastic differences between symmetric ether- and ester-linked phosphatidylcholines in their gel phase. For instance, while DPPC forms a tilted lamellar gel phase, $L_{\beta'}$, below the pretransition, DHPC shows an untilted but interdigitated (four hydrocarbon chains per head group) gel phase under the same experimental conditions. DPPC also shows a conditionally reversible, high-enthalpy, subtransition on low-temperature incubation while DHPC shows a reversible, low-enthalpy subtransition; further, ^{31}P NMR showed fast axial diffusion of DPPC down to −20 °C while this motion no longer exists for DHPC below 0 °C.

The above differences in structural behavior between ether- and ester-linked phosphatidylcholines (containing both symmetric and asymmetric hydrocarbon chains) suggest profound effects due to different chain linkage to the glycerol backbone.

Acknowledgments

We thank David Jackson and Dr. D. Atkinson for technical help and advice. We thank Irene Miller for help in preparing the manuscript.

References

Bittman, R., Clejan, S., Jain, M. K., Deroo, P. W., & Rosenthal, A. F. (1981) *Biochemistry 20*, 2790–2795.
Boggs, J. M., Stamp, D., Hughes, D. W., & Deber, C. M. (1981) *Biochemistry 20*, 5728–5735.
Chen, S. C., Sturtevant, J. M., & Gaffney, B. J. (1980) *Proc. Natl. Acad. Sci. U.S.A. 77*, 5060–5063.
Füldner, H. H. (1981) *Biochemistry 20*, 5707–5710.
Hauser, H. (1981) *Biochim. Biophys. Acta 646*, 203–210.
Hauser, H., Guyer, W., & Paltauf, F. (1981) *Chem. Phys. Lipids 29*, 103–120.
Hitchcock, P. B., Mason, R., Thomas, K. M., & Shipley, G. G. (1974) *Proc. Natl. Acad. Sci. U.S.A. 71*, 3036–3040.
Howard, B. V., Morris, H. P., & Bailey, J. M. (1972) *Cancer Res. 32*, 1533–1538.
Hui, S. W., Mason, J. T., & Huang, C. (1984) *Biochemistry 23*, 5570–5577.
Janiak, M. J., Small, D. M., & Shipley, G. G. (1976) *Biochemistry 15*, 4575–4580.
Janiak, M. J., Small, D. M., & Shipley, G. G. (1979) *J. Biol. Chem. 254*, 6068–6078.
Lee, T., & Fitzgerald, V. (1980) *Biochim. Biophys. Acta 598*, 189–192.
Levin, I. W., Thompson, T. E., Barenholz, Y., & Huang, C. (1985) *Biochemistry 24*, 6282–6286.
Luzzati, V. (1968) in *Biological Membranes* (Chapman, D., Ed.) pp 71–108, Academic Press, London and New York.
Marinetti, G. V., Erbland, J., & Stotz, E. (1959) *J. Am. Chem. Soc. 81*, 861–864.
Mattai, J., & Shipley, G. G. (1986) *Biochim. Biophys. Acta 859*, 257–265.
McDaniel, R. V., McIntosh, T. J., & Simon, S. A. (1983) *Biochim. Biophys. Acta 731*, 97–108.
McIntosh, T. J., & Simon, S. A. (1986) *Biochemistry 25*, 4058–4066.
McIntosh, T. J., Simon, S. A., Ellington, J. C., Jr., & Porter, N. A. (1984) *Biochemistry 23*, 4038–4044.
Nagle, J. F., & Wilkinson, D. A. (1978) *Biophys. J. 23*, 159–175.
Norton, W. T. (1981) *Adv. Neurol. 31*, 93–121.
Paltauf, F., Hauser, H., & Phillips, M. C. (1971) *Biochim. Biophys. Acta 249*, 539–547.
Popovič, M. (1965) *Hoppe-Seyler's Z. Physiol. Chem. 340*, 18–23.
Ranck, J. L., Keira, T., & Luzzati, V. (1977) *Biochim. Biophys. Acta 488*, 432–441.
Rouser, G., & Yamamoto, A. (1968) *Lipids 3*, 284–287.

Ruocco, M. J., & Shipley, G. G. (1982a) *Biochim. Biophys. Acta 684*, 59–66.
Ruocco, M. J., & Shipley, G. G. (1982b) *Biochim. Biophys. Acta 691*, 309–320.
Ruocco, M. J., Siminovitch, D. J., & Griffin, R. G. (1985a) *Biochemistry 24*, 2406–2411.
Ruocco, M. J., Makriyannis, A., Siminovitch, D. J., & Griffin, R. G. (1985b) *Biochemistry 24*, 4844–4851.
Schwarz, F. T., Paltauf, F., & Laggner, P. (1976) *Chem. Phys. Lipids 17*, 423–434.
Seddon, J. M., Cevc, G., & Marsh, D. (1983) *Biochemistry 22*, 1280–1289.
Seddon, J. M., Cevc, G., Kaye, R. D., & Marsh, D. (1984) *Biochemistry 23*, 2634–2644.
Sehgal, S. N., Kates, M., & Gibbons, N. E. (1962) *Can. J. Biochem. Physiol. 40*, 69–81.
Serrallach, E. N., Dijkman, R., de Haas, G. H., & Shipley, G. G. (1983) *J. Mol. Biol. 170*, 155–174.
Serrallach, E. N., de Haas, G. H., & Shipley, G. G. (1984) *Biochemistry 23*, 713–720.
Shannon, C. E. (1949) *Proc. Inst. Radio Eng. N.Y. 37*, 10–21.
Siminovitch, D. J., Jeffrey, K. R., & Eibl, H. (1983) *Biochim. Biophys. Acta 727*, 122–134.
Stumpel, J., Eibl, H., & Nicksch, A. (1983) *Biochim. Biophys. Acta 727*, 246–254.
Tardieu, A., Luzzati, V., & Reman, F. C. (1973) *J. Mol. Biol. 75*, 711–733.
Torbet, J., & Wilkins, M. H. F. (1976) *J. Theor. Biol. 62*, 447–458.
Vaughan, D. J., & Keough, K. M. (1974) *FEBS Lett. 47*, 158–161.
Witzke, N. M., & Bittman, R. (1986) *J. Lipid Res. 27*, 344–351.
Worthington, C. R., & Blaurock, A. E. (1969) *Biophys. J. 9*, 970–990.

Dual Pathways in Muscarinic Receptor Stimulation of Phosphoinositide Hydrolysis

David Gurwitz and Mordechai Sokolovsky*

Department of Biochemistry, The George S. Wise Faculty of Life Sciences, Tel Aviv University, Tel Aviv 69978, Israel

Received June 27, 1986; Revised Manuscript Received September 19, 1986

ABSTRACT: The relationships between phosphoinositide hydrolysis induced by various muscarinic agonists and by membrane depolarization agents were investigated in rat cerebral cortex and heart atrium slices. In both preparations, phosphoinositide hydrolysis was stimulated by a combination of carbamylcholine and membrane depolarization with 40 mM K^+ in a synergistic fashion. The synergism was more pronounced at lower external calcium ion concentrations and was sensitive to verapamil. Lower external calcium ion concentrations were required for demonstration of the synergism in heart atrium slices than in cerebral cortex slices. The carbamylcholine-induced stimulation was only partially additive with membrane depolarization via Na^+ channel gating by batrachotoxin. In addition, K^+ depolarization eliminated the sensitivity of carbamylcholine-stimulated phosphoinositide hydrolysis to the sodium channel blocker tetrodotoxin. Our results suggest that muscarinically stimulated phosphoinositide hydrolysis in rat cerebral cortex and heart atrium slices may occur by dual pathways which interact synergistically and that only one of the pathways is depolarization-dependent. Different muscarinic agonists could preferentially utilize these pathways, thus perhaps explaining their different potencies in stimulating phosphoinositide hydrolysis.

Activation of cholinergic muscarinic receptors in various tissues leads to increased hydrolysis of membrane phosphoinositides (Berridge & Irvine, 1984; Hokin, 1985). Inositol 1,4,5-trisphosphate ($InsP_3$),[1] a product of phosphatidylinositol 4,5-bisphosphate hydrolysis, functions in many instances as a second messenger for mobilization of intracellular Ca^{2+} stores, which in turn mediate the physiological response to muscarinic stimulation (Berridge & Irvine, 1984; Hokin, 1985; Berridge et al., 1982, 1983; Aub & Putney, 1985). Another product of phosphoinositide hydrolysis is diacylglycerol (DG), which activates protein kinase C (PK-C) (Kikkawa et al., 1982; Nishizuka, 1984). This enzyme is also activated by phorbol esters, which block phosphoinositide hydrolysis by activated muscarinic (Orellana et al., 1985; Vicentini et al., 1985) and other receptors (Leeb-Lundberg et al., 1985). We have recently described interactions between muscarinic receptors and the Na^+ channel ligand batrachotoxin (BTX) (Cohen-Armon et al., 1985; Cohen-Armon & Sokolovsky, 1986). Possible involvement of a sodium channel gating mechanism (or mechanisms) in the muscarinic stimulation of phosphoinositide hydrolysis and in the different potencies observed for various muscarinic agonists (Fisher & Agranoff, 1981; Brown & Brown, 1984; Brown-Masters et al., 1984; Brown et al., 1984; Fisher et al., 1984; Gonzales & Crews, 1984; Jacobson et al., 1985) is therefore implicated.

Membrane depolarization by high extracellular $[K^+]$ induces phosphoinositide hydrolysis in several neuronal tissues (Kendall

* Author to whom correspondence should be addressed.

[1] Abbreviations: BTX, batrachotoxin; TTX, tetrodotoxin; $[Ca^{2+}]_i$, intracellular calcium ion concentration; $[Ca^{2+}]_o$, extracellular calcium ion concentration; PMA, phorbol 12-myristate 13-acetate; InsP, inositol 1-phosphate; $InsP_3$, inositol 1,4,5-trisphosphate; DG, diacylglycerol; PL-C, phospholipase C; PK-C, protein kinase C; EGTA, ethylene glycol bis(β-aminoethyl ether)-*N*,*N*,*N*′,*N*′-tetraacetic acid; HEPES, *N*-(2-hydroxyethyl)piperazine-*N*′-2-ethanesulfonic acid.

0006-2960/87/0426-0633$01.50/0